

## Modeling of Cavitation Phenomenon inside a Nozzle Under High Fuel Pressure Condition

Y. Moriyoshi\* and K. Suga  
Department of Mechanical Engineering  
Chiba University  
Chiba, 263-8522 JAPAN

M. Kubota  
Toyota Motor Co.  
Susono, Shizuoka, 410-1193 JAPAN

### Abstract

Direct fuel injection system is getting popular in internal combustion engines due to the superior performance in fuel economy and power. To optimize the fuel-air mixture distribution inside the cylinder, the geometry of nozzle and the mixture formation process must be well designed. To attain this, the numerical simulation will be a good tool, but the prediction ability is not enough for the practical design. In this study, a two-phase flow of fuel and gas including cavitation inside an axi-symmetrical nozzle was evaluated to improve the prediction ability. Two kinds of cavitation model (quasi-steady dynamic bubble model and discrete bubble tracking model) are proposed and implemented into a commercial code FLUENT 6.4. As a result, the discrete bubble tracking model could obtain converged solutions even for a high differential pressure conditions between the nozzle entrance and the exit up to 100 MPa and predict the cavitation phenomenon qualitatively.

---

### Introduction

The demand for thermal efficiency and low exhaust gas emissions for internal combustion engines has become more stringent in the past years. As a consequence, studies of a direct injection diesel or gasoline engine have been carried out. Many kinds of injectors are used for direct injecting internal combustion engines, where in case of a swirl type injector the spray profile changes with the ambient gas pressure [1]. A slit-type injector on the other hand keeps a strong momentum due to fan-shaped spray characteristics [2]. Multi-hole type is used for its good controllability of the spray shape [3] and outward-opening hollow-cone type injectors are used in spray-guided systems [4].

In order to enhance the spray atomization and the following evaporation, a high injection pressure is suitable, but this also causes too strong spray penetration and cavitation inside the nozzle. Cavitation can enhance the atomization of droplets, but also causes an erosion inside the nozzle and the reduction in the coefficient of discharge. Thereby, the optimized nozzle configuration has been empirically designed. Recently, development of CFD has produced successes in designing engine geometrical configurations, such as intake pipe/port, combustion chamber and exhaust gas port/pipe. The prediction of in-cylinder air-fuel mixture distribution has not been well predicted due to ambiguities, such as initial/boundary conditions at the fuel nozzle exit and turbulence modeling for two-phase flow.

In this paper, two kinds of cavitation model (quasi-steady dynamic bubble model and discrete bubble tracking model) are proposed and implemented into a commercial code FLUENT 6.4. Evaluations of the models were made for a simple axi-symmetric nozzle flow.

### Cavitation Model

**Assumptions** - In this study, cavitation consists of spherical bubbles and each bubble grows from a quite small bubble, whose diameter is determined at a constant value of  $R_0$ , not dissolved in the liquid when the ambient pressure decreases down to the saturated pressure at that temperature. On the other hand, as the ambient pressure recovers over the saturated pressure at that temperature, the bubbles start to condense and its diameter reduces down to  $R_0$ . The initial number density of bubbles,  $N_0$  and its diameter,  $R_0$  are given as the initial conditions. The temperature of both liquid and gas phases is assumed constant. The change of mass due to phase changing is not accounted for.

---

\*Corresponding author

A commercial code of FLUENT 6.4 was used for calculations and cavitation models were implemented by the authors using User-Defined-Functions.

**Quasi-steady dynamic bubble model** - In this model, a quasi-steady change of cavitation was assumed; the variation of gas phase volume fraction was estimated just accounting for the change of bubble radius based on leigh-Plesset equation.

$$R \frac{d^2 R}{dt^2} + \frac{3}{2} \left( \frac{dR}{dt} \right)^2 = \frac{1}{\rho} \left\{ p'(R) - p_\infty(t) - \frac{4\mu}{R} \frac{dR}{dt} - \frac{2\sigma}{R} \right\} \quad (1)$$

Here,  $R$  is a diameter of bubble,  $t$  time,  $p$  ambient pressure,  $p_\infty$  pressure far away,  $p'$  pressure inside bubble,  $\mu$  viscosity,  $\sigma$  surface tension of liquid.  $p'$  can be expressed by Eq. (2).

$$p' = \left( p_{\infty 0} - p'_v + \frac{2\sigma}{R_0} \right) \left( \frac{R_0}{R} \right)^{3\gamma} + p'_v \quad (2)$$

Here,  $p_{\infty 0}$  is ambient pressure,  $p'_v$  vapor pressure,  $\gamma$  polytropic change index. Substituting Eq. (2) for (1), Eq. (3) reads.

$$R \frac{d^2 R}{dt^2} + \frac{3}{2} \left( \frac{dR}{dt} \right)^2 = \frac{1}{\rho} \left\{ \left( p_{\infty 0} - p'_v + \frac{2\sigma}{R_0} \right) \left( \frac{R_0}{R} \right)^{3\gamma} - p_\infty(t) - \frac{4\mu}{R} \frac{dR}{dt} - \frac{2\sigma}{R} \right\} \quad (3)$$

For simplification, some assumptions were made;  $p'_v$  is constant, viscosity ignorable and quasi-steady change. Thereby, the following Eq. can be read.

$$p_\infty = p'_v + \left( p_{\infty 0} - p'_v + \frac{2\sigma}{R_0} \right) \left( \frac{R_0}{R} \right)^3 - \frac{2\sigma}{R} \quad (4)$$

This can be reformulated as Eq. (5).

$$R = \sqrt[3]{\frac{p_{\infty 0} - p'_v + 2\sigma/R_0}{p_\infty - p'_v + 2\sigma/R}} \cdot R_0 \quad (5)$$

It is known that bubble starts to grow drastically as the ambient pressure decreases down to the critical pressure  $R_{CS}$ , with the critical bubble diameter,  $p_{CS}$  [5].

$$R_{CS} = R_0 \left\{ 3 \left( \frac{p_{\infty 0} - p'_v}{2\sigma} R_0 + 1 \right) \right\}^{1/2} \quad (6)$$

$$p_{CS} \equiv p_\infty(R_{CS}) = p'_v - \frac{4\sigma}{3R_{CS}} \quad (7)$$

Properly, Eq. (5) should be solved iteratively, however, the following assumption was made.

$$R = \sqrt[3]{\frac{p_{\infty 0} - p'_v + 2\sigma/R_0}{p_{CS} - p'_v + 2\sigma/R_{CS}}} \cdot R_0 \quad \text{if} \quad p_\infty \leq p_{CS} \quad (8)$$

$$R = \sqrt[3]{\frac{p_{\infty 0} - p'_v + 2\sigma/R_0}{p_\infty - p'_v + 2\sigma/R}} \cdot R_0 \quad \text{if} \quad p_\infty > p_{CS}$$

Once  $R$  is estimated, the gas phase volume,  $V_{ig}$  in each calculation mesh with a volume of  $V_i$  can be calculated by Eq. (9).

$$V_{ig} = NV_i \frac{4}{3} \pi R^3 \quad (9)$$

The number density,  $N$  was determined by Eq. (10) suggested by Alajbegovic [6].

$$N = \begin{cases} N_0 & \text{if } C \leq 0.5 \\ 2(N_0 - 1)(1 - C) + 1 & \text{if } C > 0.5 \end{cases} \quad (10)$$

Here,  $C$  is volume fraction of gas-phase in each calculation mesh. Using this assumption, the coalescence or breakup of bubbles can be modeled.

**Discrete bubble tracking model** - In this model, the transportation of bubble parcels were calculated in Lagrangian method called DPM (Discrete Phase Model) in FLUENT or DDM (Discrete Droplet Model) in common. Each 'parcel' consists of many bubbles that have the same properties, such as the diameter. Using parcels, the increase in calculation cost-up can be drastically reduced. The basic idea of this model is the same as of quasi-steady dynamic bubble model except that the transportation of bubbles is solved

The variation of bubble diameter,  $R$  is determined by Rayleigh's equation [5].

$$R \frac{d^2 R}{dt^2} + \frac{3}{2} \left( \frac{dR}{dt} \right)^2 = \frac{p - p_\infty}{\rho} \quad (11)$$

The increment of bubble diameter can be expressed by Eq. (12) using a time-step,  $\Delta t$ .

$$dR = K \sqrt{\frac{2(p - p_\infty)}{3\rho}} \cdot \Delta t \quad (12)$$

Once  $dR$  is estimated, the gas-phase volume,  $V_{ig}$  in each calculation mesh with a volume of  $V_i$  can be estimated.  $K$  is a coefficient and set at 1.0 in standard.

Comparing this model to quasi-steady dynamic bubble model, the spatial distribution of parcels can be precisely predicted as each parcel's advection is solved and the calculation stability is much better. Meanwhile, the calculation cost is much higher and the assumption of spherical bubble may not be used for some conditions because the accuracy of bubble tracking strongly affects the calculated results.

## Results and Discussion

**Calculation conditions** - In order to evaluate the cavitations models, comparisons between calculation and measurement were carried out for an axi-symmetric nozzle shown in Fig. 1. The nozzle radius at the inlet and outlet is 0.515 mm and a contracted nozzle with a radius of 0.22 mm

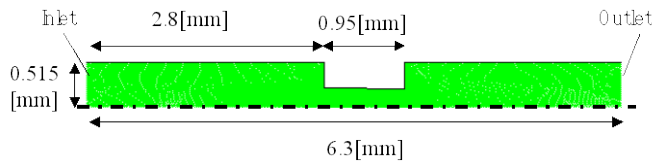


Figure 1. Configuration of an axi-symmetrical nozzle

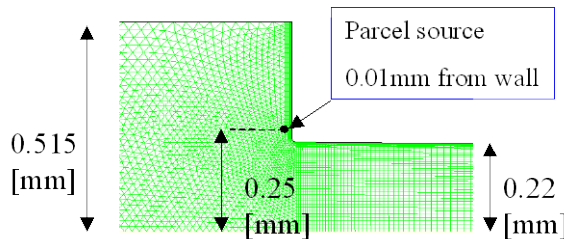


Figure 2. Location of parcel source

Table 1. Calculation conditions

Inlet pressure	Outlet pressure	$\Delta$ pressure
7.9[MPa]	3.4[MPa]	4.5[MPa]
7.9[MPa]	2.9[MPa]	5[MPa]
7.9[MPa]	1.9[MPa]	6[MPa]

Table 2. Physical properties

	Liquid phase	Gas phase
Density	830[kg/m <sup>3</sup> ]	9.4[kg/m <sup>3</sup> ]
Viscosity	0.00332 [kg/m-s]	7e-6[kg/m-s]

As the boundary condition, pressure at both the inlet and outlet was given as shown in Table 1. A standard k- $\epsilon$  turbulence model was used. Small bubbles were supplied from a source near the nozzle entrance as shown in Fig. 2. The initial bubble diameter was set at 2  $\mu$ m. The volume fraction of total gas phase was set at 0.1 %. The physical properties for the working fluids are shown in Table 2.

**Results using quasi-steady dynamic bubble model** - Figure 3 is a comparison of calculation and measurement at  $\Delta p = 5$  MPa. As the measurement was made just by taking pictures using a back light, the image is line-of-sight result and then, only the length of cavitation is available from this picture. This result demonstrates that the cavitation starting point is just nozzle entrance and disappears just nozzle exit in the experiment while it starts a little downstream and continues from the nozzle exit downstream. Thus, the prediction ability was not good and calculation was diverged for other differential pressure conditions.

**Results using discrete bubble tracking model** - Figure 4 is a comparison of calculation and measurement at  $\Delta p = 4.5, 5$  and  $6$  MPa. When  $\Delta p = 5$  MPa, the cavitation length is underestimated in the calculation. Meanwhile, as  $\Delta p = 6$  MPa in the experiment, the cavitation reaches to the end of nozzle exit and bubbles flow out near the center-axis in the expanded area. In the calculation, however, bubbles disappear downstream as condensation occurs and bubbles remain in the recirculation area near the nozzle exit in the expanded pipe where pressure is lower than saturated vapor pressure. As the length of cavitation seems to depend on the coefficient of  $K$  in Eq. (12) that determines the expansion or contraction of bubbles, the effect of  $K$  was examined.

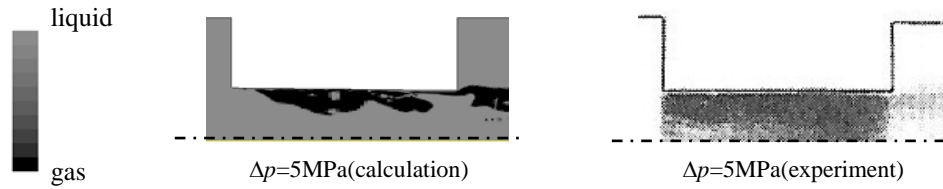


Figure 3. Results of gas-phase volume fraction for  $\Delta p= 5$ MPa condition using quasi-steady dynamic bubble model

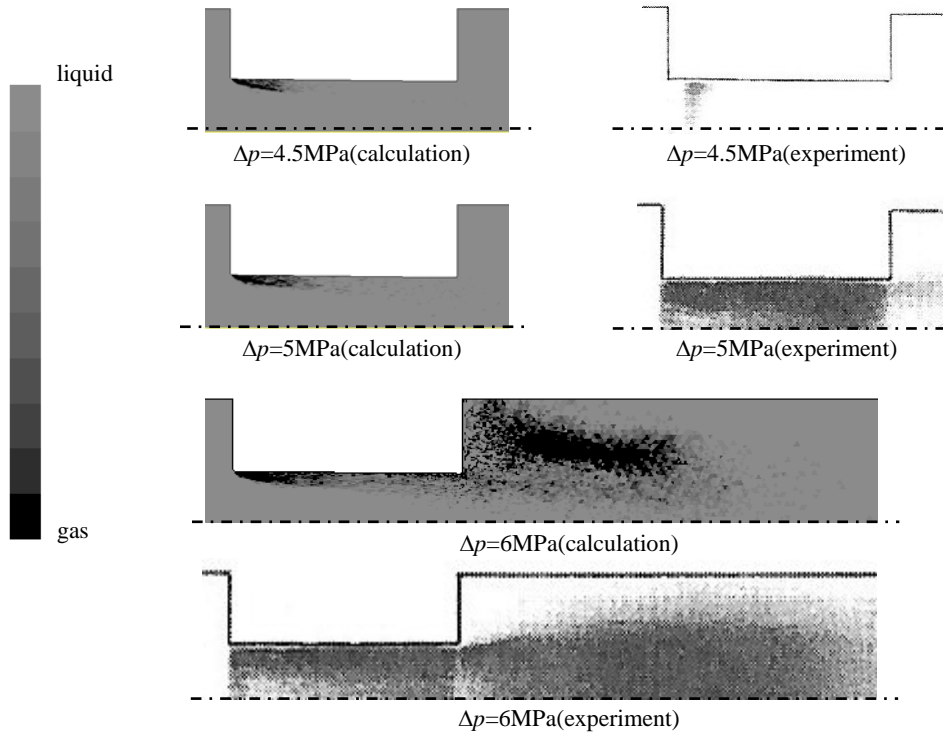


Figure 4. Results of gas-phase volume fraction for  $\Delta p= 4.5, 5$  and  $6$ MPa conditions using discrete bubble tracking model

Figure 5 shows the effect of  $K$  on cavitation formation.  $K$  is an acceleration coefficient to change the bubble diameter. Thereby, it can be expected that the cavitation length becomes long as  $K$  takes over unity during the expansion and/or it takes under unity during the contraction. However, no much difference was found in Fig. 5.

As other initial/boundary conditions, the initial bubble diameter,  $R_0$  and initial volume fraction of total gas-phase,  $V_{ig}$  were varied to see the effect. Figure 6 shows that  $R_0$  was varied from 1 to 4  $\mu\text{m}$  while  $V_{ig}$  from 0.05 to 0.2 %. Comparing the results to each other, not much difference was found. Thereby, these parameters are not so sensitive to the predictions. This is favorable for predictions.

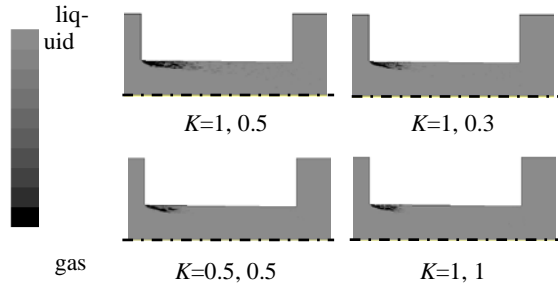


Figure 5. Effect of  $K$  on cavitation formation

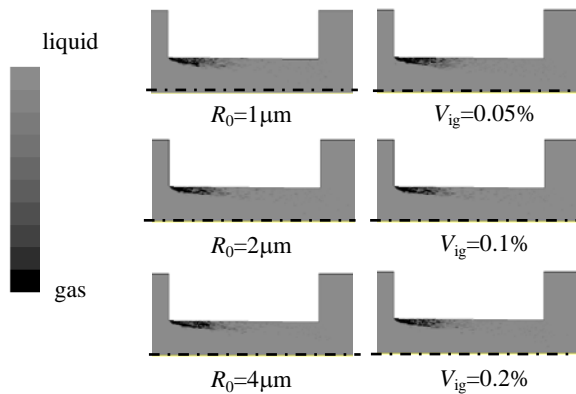


Figure 6. Effect of initial condition on cavitation formation

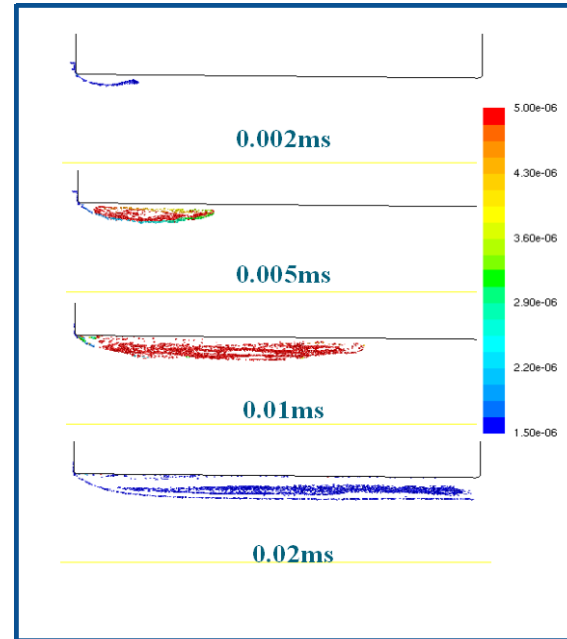


Figure 7 Temporal variation of cavitation bubbles at  $\Delta p = 100 \text{ MPa}$

Figure 7 shows temporal variation of bubbles with the bubble diameter at  $\Delta p = 100 \text{ MPa}$ . The bubbles are quickly transported on the flow.

## Conclusion

A two-phase flow of fuel and gas including cavitation inside an axi-symmetrical nozzle was evaluated to improve the prediction ability. Two kinds of cavitation model (quasi-steady dynamic bubble model and discrete bubble tracking model) are proposed and implemented into a commercial code FLUENT 6.4. As a result, discrete bubble tracking model that includes the transportation of bubble parcels in Lagrangian method and the temporal change of bubble diameter using Rayleigh's expression could obtain converged solutions even for high differential pressure between the nozzle entrance and the exit up to 100 MPa and predict the cavitation phenomenon qualitatively compared to the experimental results. Moreover, the sensitivity of the initial bubble diameter and initial volume fraction of total gas phase was found not large.

## References

1. Y. Iwamoto, Development of gasoline direct injection engine, SAE Paper 9712902
2. M.Koike, A.Saito, T.Tomoda and Y.Yamamoto, Research and Development of a New Direct-Injection Gasoline Engine, SAE Paper 2000-01-0530
3. T.Honda, M.Kawamoto, H.Katashiba, M.Sumida, N.Fukutomi, K.Kawajiri, A Study of Mixture Formation and Combustion for Spray-Guided Disi, SAE Paper 2004-01-0046
4. M.Skoqsberg, P.Dahlander, I.G.Denbratt, Spray Shape and Atomization Quality of an Outward-Opening Piezo Gasoline DI Injector, SAE Paper 2007-01-1409
5. Y. Kato, "Cavitation (New Edition)" (in Japanese) Maki Syoten, (1999) 30.
6. A. Alajbegovic, et al., Experimental Thermal and Fluid Sci. 26 (2002) 677.